Ab initio calculations of Si, As, S, Se, and Cl adsorption on Si(001) surfaces

Peter Krüger and Johannes Pollmann
Institut für Theoretische Physik II, Universität Münster, D-4400 Münster, Germany
(Received 28 July 1992)

Optimal adsorption geometries and respective surface band structures for monolayers of group-IV to group-VII adatoms on semi-infinite Si(001) substrates have been calculated from first principles using a self-consistent total-energy scheme. The calculations are based on the local-density approximation and employ nonlocal, norm-conserving pseudopotentials together with Gaussian orbital basis sets. The semi-infinite geometry of the substrate is properly taken into account by employing our scattering theoretical method together with one-particle Green's functions. Chemical trends in the adsorption of Si, As, S, Se, and Cl monolayers on Si(001) are discussed. Our calculational scheme treats all these adlayers on equal footing. The clean Si(001)-(2×1) surface shows an asymmetric dimer reconstruction which is 0.14 eV per dimer lower in energy than the respective optimal symmetric dimer configuration. An As adlayer gives rise to symmetric As dimer chains at the chemisorbed surface which run orthogonal to the former Si dimer chains at the clean surface. The substrate atoms in this As:Si(001)-(1×2) system reside close to the lattice sites of the Si bulk crystal. Adsorption of a monolayer of group-VI adatoms is found to restore the substrate surface in its ideal, truncated bulk configuration and to passivate the surface. S or Se adlayer atoms are adsorbed in bridge positions above the surface in sites very close to the lattice positions of the continued bulk lattice and form S:Si(001)-(1×1) and Se:Si(001)-(1×1). A Cl adlayer, finally, gives rise to Cl:Si(001)-(2×1). The adatoms adsorb on top of the dangling bonds of a (2×1)-reconstructed substrate surface showing symmetric Si dimers. The results of our structure optimizations are in excellent agreement with a whole body of experimental data. The calculated electronic structure for Si(001)-(2×1) and for As:Si (001)-(1×2) shows very good agreement with angle-resolved photoemission spectroscopy (ARPES) data. Well-ordered S:Si(001)-(1×1) and Se:Si(001)-(1×1) surfaces have not been fabricated successfully, so far. Our calculated electronic surface band structure for Cl:Si(001)-(2×1) does not yet easily allow for an obvious interpretation of available ARPES data.

I. INTRODUCTION

Investigations of the chemisorption of adatoms on silicon surfaces are important both technologically, in the context of passivation, doping, heteroepitaxy, and growth, and for fundamental physical reasons. One of these reasons is a better understanding of bonding and reconstruction at semiconductor surfaces. The Si(001) surface has emerged as a prototype system in experimental and theoretical studies. The reconstruction of the clean surface occurs in order to reduce the number of broken Si dangling bonds. Adsorption of adatoms can change the surface reconstruction in many ways by formation of new bonds. It is instructive to study these effects as a function of the number of valence electrons and the atomic radii of the chemisorbed atoms to find out chemical trends in bonding characteristics. In this paper we will discuss the structural and electronic properties of ordered Si, As, S, Se, and Cl monolayers on the Si(001) surface in detail on the basis of first-principles Green's functions calculations carried out for semi-infinite systems in the framework of the local-density approximation (LDA). These particular adsorbed species of group-IV to group-VII adlayers have been chosen for a number of reasons: (a) they allow one to study the effect of increasing number of valence electrons per adatom ranging from four electrons at the clean surface (covalent bonding) through five and six electrons for As, S, and Se adlayers (heteropolar bonding) up to seven electrons in the case of a Cl adlayer (ionic bonding); (b) their structural and electronic properties have been investigated recently by low-energy electron diffraction (LEED), core-level spectroscopy, and angle-resolved photoemission spectroscopy (ARPES);[1–4] and (c) they are of particular technological interest in manufacturing electronic devices. For example, the reaction of chlorine gas is known to be useful in dry etching and photo-surface cleaning. Furthermore, in heteroepitaxy of compounds on elemental semiconductors (e.g., GaAs on Si or ZnSe on Si) the initial stages of the process are of predominant importance, and, for instance, the adsorption of As on the Si surface is usually the first step in epitaxial growth of GaAs on Si.

The clean Si(001) surface can be viewed as an ideal, bulk-terminated semi-infinite substrate with an adlayer of Si atoms. This adlayer shows the strongest reconstruction effects, while the substrate layer atoms show much smaller structural changes with respect to the bulk lattice. The clean surface shows a strong (2×1) reconstruction in the LEED pattern, as had been shown by Schlier and Farnsworth 33 years ago.[5] In addition to this, energetically weaker reconstructions with larger unit cells [$c(4\times2)$, $p(2\times2)$] have been reported.[6] Schlier and Farnsworth have explained their observations by the existence of dimers, created by pairing of nearest-neighbor surface atoms. Several models for the (2×1) reconstruction have since been proposed.[7] There is now general

agreement that dimers are the main building blocks of the reconstructed surface. But it is still an open question whether the dimers are symmetric or buckled, as suggested by Chadi[8] on the basis of the results of his empirical tight-binding calculations. The picture of asymmetric dimers was supported experimentally by ion-scattering measurements[9,10] and LEED experiments.[11] *Ab initio* total-energy calculations also favored asymmetric dimers.[12] This model was questioned by Pandey,[13] who proposed a defect model based on symmetric dimers. Various calculations carried out later within the LDA framework yielded contradictory results, preferring either asymmetric dimers[14–16] or symmetric dimers.[17–20] Many of these results[12–18] were obtained using the same ingredients: first-principles pseudopotentials, slab models, and a plane-wave basis set. Small calculational differences (basis-set convergence, sampling of $\mathbf{k}_{\parallel}$ points, etc.) lead to different results due to the fact that the energy difference per dimer between the asymmetric and the symmetric structures is relatively small. It was found to be on the order of 0.02–0.1 eV in Refs. 12–18. A coexistence of asymmetric and symmetric dimers with about 10% surface defects was observed in scanning-tunnel-microscopy (STM) experiments[21] carried out at *room temperature.* Recent STM experiments[22] clearly show that at 120 K the number of buckled dimers increases at the expense of symmetric dimers. We report in this paper total-energy calculations for semi-infinite Si(001)-(2×1) using *ab initio* pseudopotentials and a basis set of localized Gaussian orbitals. Our results show that buckled dimers are energetically favored over symmetric ones by 0.14 eV per dimer.

Adsorption of As on Si(001) changes the reconstruction of the clean surface from (2×1) to (1×2), as shown by Bringans *et al.*[2] These authors have worked out a structural model from their experimental findings and from total-energy calculations for a ten-layer slab. In their model As atoms form *symmetric dimers* on top of the Si(001) surface. The dangling-bond orbitals of the As atoms give rise to dangling-bond bands, whose dispersion has been measured.[2] In addition to these states the experiment shows strong resonances in the energy region from −2 to −4 eV. The origins of these resonances could not reliably be assigned in Ref. 2 due to the slab geometry used in the calculations. The scattering theoretical method which we have used for the studies presented in this paper allows a determination of surface resonances with high spectral resolution. We have clearly identified these states as originating from the dimer bonds. The calculated dispersions of the resonances are in very good agreement with the measured features. Our computations lead to an equilibrium configuration of the surface in accordance with the model presented by Northrup (see Ref. 2). Each atom turns out to be fully coordinated in this (1×2) geometry.

Adsorption of S or Se on Si(001) shows particularly interesting structural properties in that a monolayer of these adatoms completely removes the substrate reconstruction. So far, this is a result of our theory only. However, for S adsorbed on Ge(001), Weser *et al.*[23] reported already the preparation of a well-ordered Ge(001)-(1×1) configuration. Core-level spectroscopy investigations,[23] photoemission measurements,[24] and total-energy minimization calculations[25] for that system have identified a bonding geometry with the sulfur atoms residing in bridge positions above the Ge atoms of the topmost substrate layer. For S or Se monolayers on Si(001), that particular configuration has not been obtained experimentally so far. For S:Si(001), no ordered adlayer could be observed.[26] For Se:Si(001), Bringans and Olmstead[3] reported a replacement of the (2×1) LEED pattern of the clean reconstructed surface by a (1×1) pattern for a submonolayer film of Se on Si (001) after annealing to 550 °C. We note in passing that Bringans and co-workers[27,28] have demonstrated surface restoration and passivation beautifully by adsorbing As monolayers on Si and Ge (111) surfaces. For ordered monolayers of S or Se on Si(001) we have calculated optimal surface configurations, binding energies, and the surface electronic structure. The results will be presented in this paper and will be discussed in comparison with our earlier results for S:Ge(001)-(1×1).[25,29]

Adsorption of Cl on Si(001) retains the (2×1) reconstructed substrate surface. It can be expected, however, from simple chemical arguments that the adsorption of a Cl monolayer leads to symmetric dimers in the Si substrate surface layer with the Cl adatoms saturating the partially filled Si dimer dangling bonds. The resulting surface structure should be very similar to the geometry of the hydrogen-chemisorbed Si(001) surface.[1,30,31] This model is supported by early photoemission measurements of Rowe and Margaritondo[32] and recent surface-extended x-ray-adsorption fine-structure (SEXAFS) investigations by Thornton *et al.*[33] Cl:Si(001)-(2×1) has also been studied experimentally by low-energy electron-energy-loss spectroscopy (LEELS)[34] and thermal-desorption measurements.[35] In 1990, Johansson *et al.*[4] carried out extensive ARPES measurements on Cl:Si(001)-(2×1). They have detected numerous Cl-induced states in an energy region from −5 to −10 eV below the Fermi level. However, an unambiguous determination of the origin of these states was difficult due to the lack of detailed theoretical results on Cl:Si(001)-(2×1). Very recently, Craig and Smith[36] computed the structural and electronic properties of the Cl-covered Si(001) surface using the semiempirical modified intermediate neglect of differential overlap (MINDO) technique. Their calculations, carried out for a 10-layer slab, show that the symmetric Si-Si dimer configuration with chemisorbed Cl atoms, as described above, corresponds to a local minimum in configuration space. Moreover, they identified another surface topography with a lower total energy as compared to the above-mentioned dimer configuration. In that geometry, the Cl atoms are adsorbed in two different bridge positions, which we will discuss in more detail below. Craig and Smith have published integrated densities of states for both configurations.[36]

The purpose of this paper is to present theoretical results for the clean reconstructed Si(001) surface and for As, S, Se, and Cl adsorption on Si(001) as obtained under identical numerical conditions for semi-infinite systems in

order to contribute to a detailed understanding of the chemical trends in the changes of bonding and reconstruction when monolayers ranging from group-IV to group-VII adatoms are adsorbed on Si(001).

The paper is organized as follows. In Sec. II we briefly describe the theoretical method. Section III presents and discusses theoretical results for the clean and chemisorbed Si(001) surface and compares them with available experimental data. Our conclusions drawn from this study are given in a summary in Sec. IV.

II. METHOD OF CALCULATION

The calculations have been carried out within the LDA[37,38] using our self-consistent scattering theoretical method.[39,40] This approach solves the Kohn-Sham equations[41] for a semi-infinite system self-consistently by treating the ordered clean, reconstructed, or adsorbate-covered surface as a two-dimensionally periodic perturbation of a bulk crystal. Due to the electronic screening this perturbation is extremely localized perpendicular to the surface. To represent this localized perturbation, the wave functions are expanded in terms of a linear combination of atomic orbitals and the corresponding secular equation is solved by a calculation of its inverse or Green's function. The Green's function contains the full information on the electronic one-particle spectrum of the semi-infinite surface system. Optimal surface configurations are determined by minimizing the total energy. This is achieved by calculating the forces acting on the atoms in the area of the perturbation and by a simultaneous relaxation of ionic coordinates and electronic-charge density until the forces are vanishingly small. The formal treatment and the computational procedure have been described in detail in Refs. 40 and 42. Here we address a few technical points only, which are specific to the calculations reported in this paper. In our basis set we use 20 Gaussian orbitals (s, p, d, s^*) per atom. An additional ten Gaussian orbitals are localized at each surface atom to take the spatial extent of the wave functions into vacuum into account.[43] We have used norm-conserving, nonlocal pseudopotentials of Bachelet, Hamann, and Schlüter[44] together with the Ceperley-Alder[45] form of exchange-correlation (XC) energy, as parametrized by Perdew and Zunger.[46] In addition, to this we have carried out calculations using the separable form of the pseudopotentials as tabulated by Stumpf, Gonze, and Scheffler.[47] A significant reduction of the numerical effort in the calculation of the matrix elements is achieved by these pseudopotentials. The resulting structural and electronic properties are nearly identical for both types of pseudopotentials. Bond lengths differ by less than 0.5% and surface-band positions differ by less than 0.1 eV. Brillouin-zone integrations in the bulk calculation have been carried out using 10 special $\mathbf{k}$ points. The bulk Green's function has been computed by summing over 301 $\mathbf{k}_\perp$ values [see Eq. (40) in Ref. 40]. Surface Brillouin-zone integrations have been carried out using eight special $\mathbf{k}_\parallel$ points in the full (2×1) cell. The number of special $\mathbf{k}_\parallel$ points was extended to 32 for the determination of the final optimized structures. Charge redistributions have been taken into account within the first five layers using a grid with a spacing of 0.25 Å. We have calculated the binding energy E_{bind} for ordered monolayers from

$$E_{\text{bind}} = E_{\text{chemi}} - E_{\text{Si(001)}} - E_{\text{atom}} ,$$

where E_{chemi} denotes the energy of the chemisorption systems, $E_{\text{Si(001)}}$ is the energy of the clean, (2×1)-reconstructed Si(001) surface, and E_{atom} has been estimated from a total-energy calculation for the free atom using the same basis set as in the Green's functions calculation. The spin-polarization energy of the free atoms has been separately computed for spin-polarized pseudoatoms using the energy functional of Ref. 46.

III. RESULTS AND DISCUSSION

Let us first address a few important quantities of the underlying Si bulk crystal. Table I represents the equilibrium lattice constant, the bulk modulus, and the cohesive energy as they result from our calculation. To calculate these properties, we have employed both the Ceperley-Alder (CA) and Wigner (W) forms of the exchange-correlation energy functionals. The equilibrium lattice constant and the bulk modulus are obtained from the total energy, calculated as a function of lattice constants, and the Murnahghan equation of state[48] has been employed. The cohesive energy has been calculated from the difference between the energy per Si atom in the bulk solid and the energy of a spin-polarized pseudoatom. In each case, the spin-polarized energy functional of Ref. 46 has been used. In our results the bulk lattice constant is underestimated by 1.1% (0.4%) when the Ceperley-Alder (Wigner) XC functional is used. Plane-wave calculations carried out by Zhu, Fahy, and Louie[49] with an energy cutoff $E_{\text{cut}} = 18$ Ry ($\hat{=}350$ plane waves) yield slightly better results (see Table I). We note in passing that the less-well-founded Wigner form of exchange and correlation energy[50] happens to yield lattice constants, bulk moduli, and cohesive energies in even better agreement with experiment than the Ceperley-Alder XC functional.

A. Clean Si(001)-(2×1) surface

We have carried out minimizations of the total energy to optimize the structure of the clean Si(001) surface

TABLE I. Calculated bulk properties of Si using Ceperley-Alder (CA) (Ref. 46) and Wigner (W) (Ref. 50) forms of exchange-correlation potentials in comparison with results of the plane-wave (PW) calculations of Ref. 49. The experimental values are from Ref. 51.

Calculation	Exchange correlation	Lattice constant (Å)	Bulk modulus (Mbar)	Cohesive energy (eV/atom)
present	CA	5.37	1.15	5.03
PW	CA	5.38	1.00	5.24
present	W	5.41	1.00	4.67
PW	W	5.43	0.90	4.95
experiment		5.43 (0 K)	0.99	4.63

within the (2×1) symmetry. Minimization without any restrictions leads to asymmetric dimers with a bond length of 2.25 Å and a buckling angle of 19°. The corresponding values of Kobayashi *et al.*[16] are 2.27 Å and 14°. Dabrowski and Scheffler[15] have reported a buckling angle of 15° for the optimized structure. Restricting the atomic degrees of freedom to symmetric configurations we find a stable configuration with a dimer bond length of 2.25 Å. The symmetric geometry is 0.14 eV per dimer higher in energy than the asymmetric geometry. We have repeated the optimization procedure using several start geometries. In each case we arrived at the same minimum in configuration space.

The surface band structure following from our Green's-function calculation for the optimized asymmetric structure is shown in Fig. 1. The shaded area represents the projected bulk band structure. We have labeled the various states according to their physical origin and character. The states S_1-S_5 are predominantly *s*-like. The bands B_1-B_5 stem from back-bond states. They are strongly *p*-like with small *s* and *d* admixtures. The dimer bond gives rise to the band D_{di}. In the fundamental gap, there are two bands labeled D_{up} and D_{down}, which originate from the dangling bonds at the up and down atoms of the surface dimers, respectively. The surface is semiconducting with an indirect gap of 0.15 eV. This gap is very sensitive to the buckling angle. In the case of symmetric dimers the Si(001) surface turns out to be metallic in our calculations, in contrast to experimental findings.[52]

Figure 2 shows a small section of the calculated surface band structure along the [100] direction from Γ to J' for the asymmetric dimer configuration in comparison with

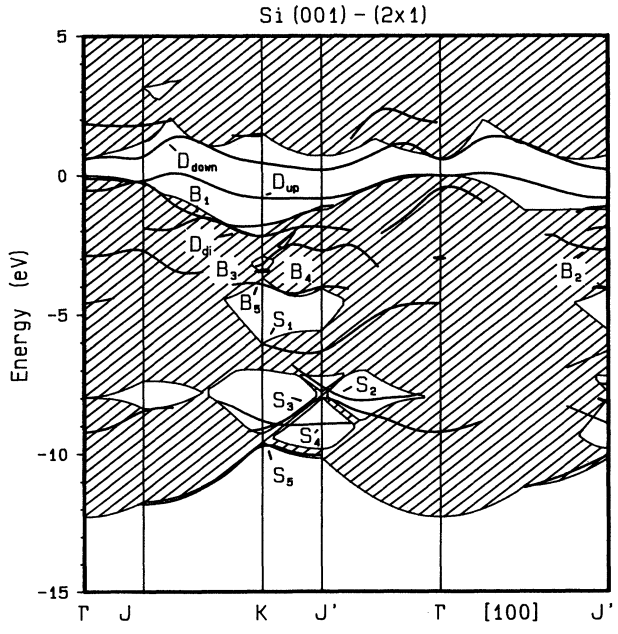

FIG. 1. Surface band structure of the clean Si(001)-(2×1) surface in the asymmetric dimer configuration. The shaded area represents the projected bulk band structure.

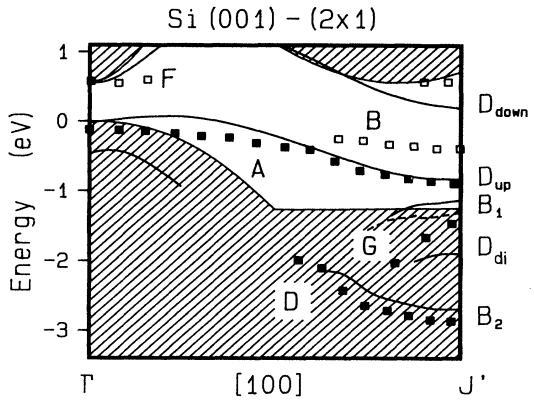

FIG. 2. Self-consistently calculated electronic surface bands in comparison with experimental surface band structure (*A,B,D,F,G*) of Ref. 53. Open (solid) symbols denote weak (strong) surface structures.

ARPES data by Johansson *et al.*[53] The [100] direction is the diagonal of the surface Brillouin zone and it is equivalent for the (2×1) and (1×2) reconstructions. Measuring along this direction in general avoids multidomain effects in the spectra. Five features have been detected for $\mathbf{k}_{\parallel}$ vectors along this direction in an energy range of 5 eV below the Fermi level, which was estimated to be at 0.6 eV above the top of the valence bands.[53] The labeling of the experimental results *within* the plot refers to the nomenclature of Ref. 53. The labeling on the right-hand margin refers to the theoretical identification of the bands according to Fig. 1. The measured surface-state band *A* can be interpreted as the dangling-bond band D_{up} of the asymmetric dimer model, as is evident from the common dispersion and energy position of *A* and D_{up}, respectively. The calculated bandwidth of 1.0 eV is somewhat larger than the bandwidths measured by various groups (0.6,[54] 0.7,[53] and 0.8 eV[55]). The measured band *D* agrees well in dispersion and energy position with the calculated back-bond resonance B_2. Johansson *et al.* have claimed a strong p_z character for this resonance on the basis of its polarization dependence in the ARPES data. The structure *D* is a very pronounced feature (see Fig. 8 of Ref. 53) in the photoemission spectrum. The orbital character of the calculated B_2 state is in very good accordance with this finding. The related charge-density contours show a density maximum spilling out into vacuum in the *z* direction between the dimers, explaining why this bond occurs as a strong feature in the data. A very similar state has been observed and calculated for the clean Ge(001)-(2×1) surface.[56] The measured band *G* cannot be interpreted free from doubt as a surface resonance on the basis of the experimental observations.[53] Comparing with our theoretical results it neither coincides with the B_1 band nor with the dimer band D_{di}. Our results reveal that there is a strong *bulk resonance* in this energy region. We have indicated it in the figure by a dashed line. At J' its energy position happens to nearly coincide with the measured structure *G*. But this reso-

nance cannot fully explain the measured band, since its dispersion is much smaller than that of the measured band G. The calculated dimer-bond state D_{di} and the back-bond state B_1 have not been resolved in experiment, probably due to their particular wave-function character. Two further measured bands B and F are shown in the figure. The structure B is only seen near J' and it has a very weak dispersion. It could be detected only near J' by using light which was polarized perpendicular to the plane of incidence in order to suppress the strong emission of the dangling-bond state. In the other parts of the surface Brillouin zone it cannot be discerned from the dangling-bond emission. This state cannot be interpreted on the basis of models for a well-ordered (2×1) dimer-reconstructed surface. The results of STM measurements lead to the conclusion that there is a coexistence of asymmetric dimers, symmetric dimers, and defects at real Si(001) surfaces. Especially at lower temperatures, there are large domains with higher-order reconstructed [$c(4\times2)$ or $p(2\times2)$] asymmetric dimers.[22] Zhu, Shima, and Tsukada[14] have studied models of dimers which are arranged in $p(2\times2)$ or $c(4\times2)$ periodicities in a pseudopotential slab calculation. The resulting dispersion of their dangling-bond bands is consistent with the dispersion of the measured band B. However, a detailed comparison between energy dispersions of the measured bands with those calculated in Ref. 14 is difficult due to the large slab-induced splittings of the surface states in the calculations and due to the fact that the structure B could not be resolved experimentally in the whole Brillouin zone.

The origin of the state F cannot be clearly identified from a band-structure calculation for the (2×1) structure, as well. It may be argued that the emission of F near Γ and J' results from the dangling-bond band D_{down}, which has been partially filled by n doping. But the energetic positions of F at Γ and J' are roughly the same in contrast to the calculated dispersion of D_{down}. The dangling-bond band D_{down} is 0.3 eV lower in energy at J' with respect to the value at Γ. Our results for the symmetric dimer model show much less agreement with the experimental data, and they cannot explain features B and F as well.

We conclude that the gross features in the photoemission spectra of a Si(001) surface showing a good single-domain (2×1) LEED pattern are in good agreement with the calculated electronic structure resulting for the asymmetric dimer model. The LEED and photoemission experiments measure predominantly properties which are averaged over large parts of the crystal surface. However, there is a high degree of local imperfections of the surface clearly detected by STM.[21,22] They give rise to additional features in the electronic spectrum which are detected by modern high-resolution ARPES.[52,53] For a detailed theoretical investigation of these effects, calculations for point perturbations at surfaces, e.g., Green's-function computations,[57–59] have yet to be carried out.

Finally, we mention that the absolute energy position of our calculated bands is slightly higher ($\Delta E=0.2$ eV) than that of the measured bands. This deviation is a well-known shortcoming of LDA calculations and it has been observed for many other clean and adsorbate-covered surfaces as well. A rigid shift of the calculated bands by $\Delta E=0.2$ eV down in energy would show even better agreement between theory and experiment.

B. As:Si(001)-(1×2)

The equilibrium lattice configuration resulting from our total-energy minimization for an ordered monolayer of As on the Si(001) surface within the (1×2) symmetry is shown in Fig. 3(a) together with the total valence charge density of the As-As dimer above the surface. We obtain symmetric As dimers with a dimer bond length of 2.52 Å. This relatively large dimer bond length is the

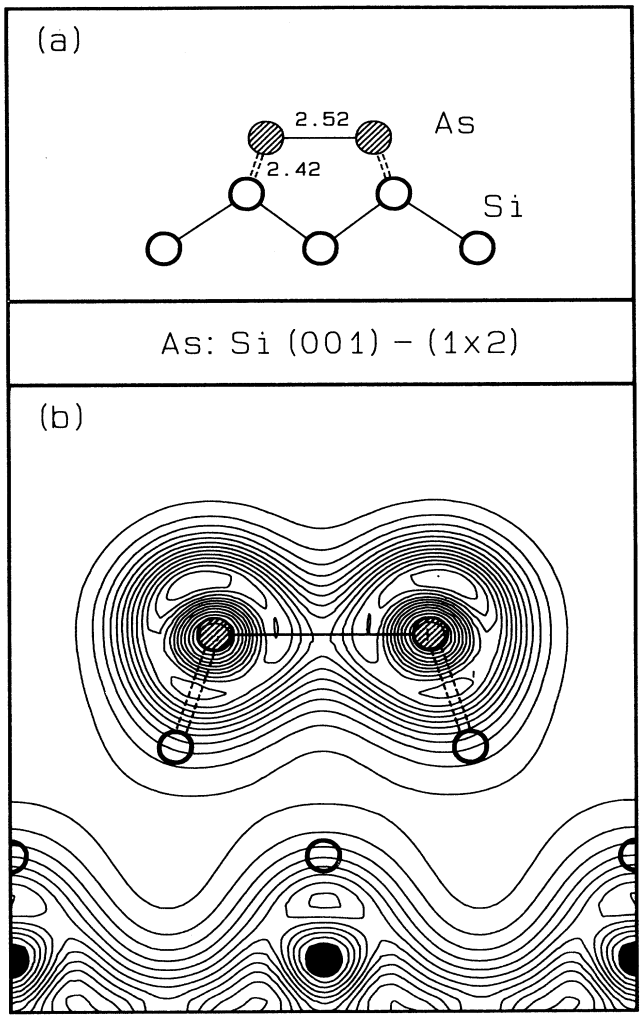

FIG. 3. (a) Side view of the As:Si(001)-(1×2) surface. The bond lengths are given in angstroms. (b) Total valence charge-density contours of As:Si(001)-(1×2) plotted in a [001]-[110] plane. Bonds in the drawing plane are plotted as solid lines while bonds that form an angle with the drawing plane are given by dashed lines. Open circles denote atoms which are not located within the drawing plane.

reason why no pronounced bond charge in the dimer occurs. The Si-As back-bond length is 2.42 Å. All Si atoms are fourfold coordinated and the As atoms are threefold coordinated. In a simple picture the adsorption process can be interpreted as a breaking of Si-Si dimers by the As atoms which form As-As dimers in the perpendicular direction. This gives rise to a rotation of the LEED pattern from (2×1) for the clean surface to (1×2) for the As-covered surface. Such a rotation was observed, indeed, for single-domain surfaces by Bringans *et al.*[54] This holds for substrate temperatures lower than 400 °C. For temperatures between 400 and 700 °C the surface reconstruction remains (2×1) after As adsorption, while at higher temperatures single-layer, double-layer, and multilayer steps have been observed.[60] Recently, Alerhand *et al.*[61] studied the structural properties of As:Si(001) surfaces with double-layer steps by carrying out slab calculations within the LDA for unit cells containing up to 120 atoms. They have shown that an As:Si(001) surface with double-layer steps has a stable and a metastable configuration, which are rotated by 90° with respect to each other.

In Fig. 4 we show the surface band structure for a well-ordered As monolayer on Si(001), as resulting from our calculations, and in Fig. 5 we show the charge-density contours of a few representative states in order to highlight the orbital character of some of the surface features. We have labeled the bands in Fig. 4 according to their physical origin. There are two As-induced *s*-like states. Their symmetric combination S_1 resides in energy below the bottom of the Si valence bands due to the fact that the As potential is more attractive than the Si potential. The antisymmetric combination S_2 occurs as a strong resonance in the lower projected bulk valence bands. The back-bond states B_1–B_3 are mainly Si *p*-like. Energetically, they reside near the edges of the projected valence–band structure, reflecting the fact that there are small changes only in the binding configuration of the topmost Si substrate layers with respect to the bulk configuration. As one example of these back-bond states, Fig. 5(a) shows the energy- and wave-vector-resolved charge density of B_1 at J'. The As dimer bond gives rise to two states D_{di} and D^*_{di} in the energy range from −2 to −4 eV. By an inspection of the charge-density contours of D_{di} shown in Fig. 5(b), we recognize that the charge-density maxima are not exactly along the interconnection line between two neighboring As atoms but spills out into vacuum. This result differs from the respective charge density of the clean Si(001)-(2×1) surface due to the fact that the As-As dimer-bond length of 2.52 Å is 10% larger than the Si-Si dimer-bond length (2.25 Å). The most prominent features in the calculated electronic spectrum are the symmetric (D) and antisymmetric (D^*) combinations of As dangling-bond states. Their charge densities at $\Gamma J'/2$ are shown in Figs. 5(c) and 5(d), respectively. The splitting in energy between these two states is rather small. Both bands are completely filled in this binding configuration, leading to a semiconducting surface in agreement with experiment.

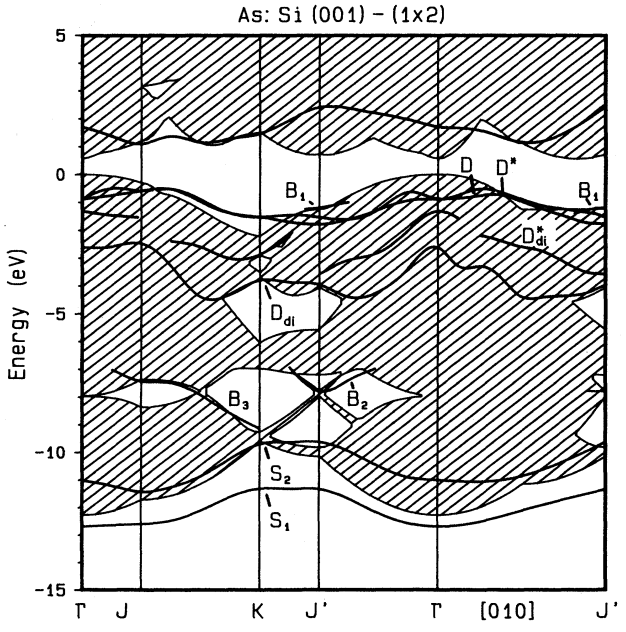

FIG. 4. Surface band structure of As:Si(001)-(1×2).

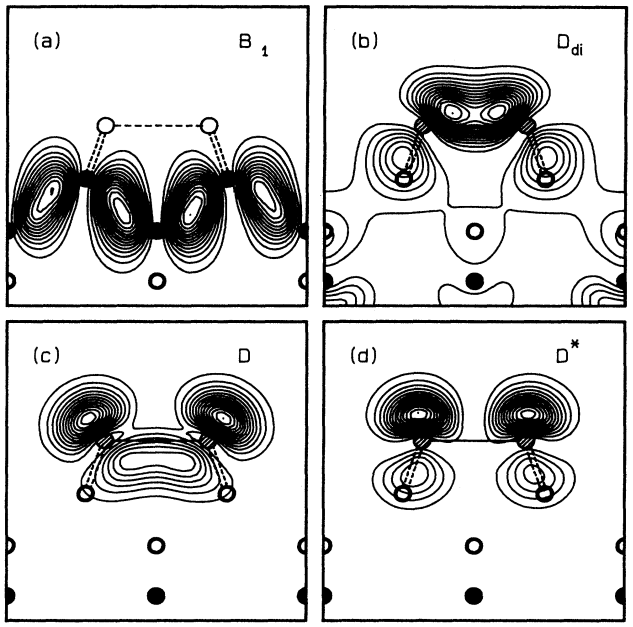

FIG. 5. Energy-resolved charge-density contours of the B_1 and D_{di} state at J', and of D and D^* at $\Gamma J'/2$ for As:Si(001)-(1×2). (b)–(d) are plotted in the [001]-[110] plane containing the As-As dimer. (a) is plotted in a [001]-[110] plane shifted by $a_0 \cdot \sqrt{2}/4$ in $[\bar{1}10]$ direction with respect to (b).

Figure 6 shows the results of ARPES measurements carried out by Uhrberg *et al.*[62] along the [010] direction from Γ to J' in comparison with the bands resulting from our calculations. Again, no energy shifts have been applied. Comparing the dispersion and the relative energet-

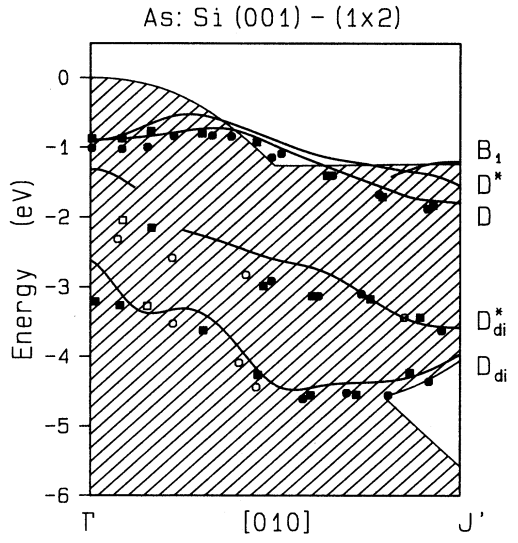

FIG. 6. Small section of the surface band structure of As:Si(001)-(1×2) in comparison with experimental data of Ref. 63. Data points have been obtained with 21.2 (eV) (●) and 25.0 eV (■). Open symbols denote weak structures.

ic position of calculated bands and measured features there is strong evidence that the observed bands in this energy region are the dimer-bond bands D_{di} and D^*_{di}. The corresponding charge densities have a strong p_z part [see, e.g., Fig. 5(b)] which is probed most efficiently by the experimental setup used in Ref. 62. We note in passing, that in the case of the clean Si(001)-(2×1) surface, on the contrary, there has been no indication for a detection of the dimer state (see, e.g., Fig. 2), probably because in that case the dimer state has only a very weak p_z contribution. The most dominant structure in the photoemission spectrum (Fig. 3 in Ref. 62) can be identified with the

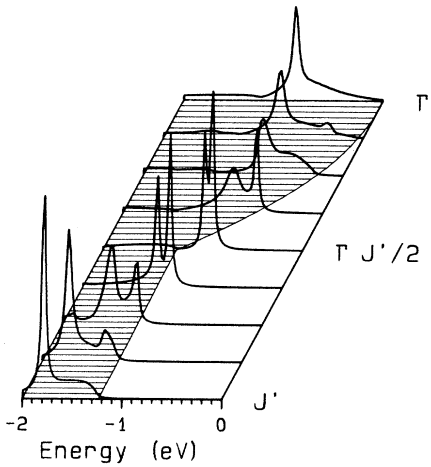

FIG. 7. Wave-vector-resolved layer density of states for As:Si(001)-(1×2) along [100] from Γ to J'. The shaded area represents the projected bulk band structure.

dangling-bond states D and D^*. The experiment shows a small splitting between D and D^* for different photon energies only. Comparing theory and experiment one should keep in mind that the dangling-bond states are given as localized states only in the gap. In the energy region of the projected band structure they become resonances and are broadened by an interaction with the underlying bulk bands. This is shown in Fig. 7 where the p_z part of the layer density of states along [010] from Γ to J' is plotted. At Γ there is one dominant peak with a broad shoulder. A second peak at higher energies increases for larger $\mathbf{k}_{\|}$. Near $\Gamma J'/2$ both states become localized with a splitting of 0.1 eV. Approaching J', the peak at higher energies broadens and decreases, while the lower peak remains sharp and shifts down in energy. Due to the limited experimental resolution the small splitting of the peaks cannot clearly be observed. The Si-Si back-bond state B_1 [see also Fig. 5(a)] has not been detected. This is not surprising since the corresponding wave functions have their maxima between the second and third layers. The results of our calculations thus nicely confirm the symmetric dimer model worked out by Uhrberg *et al.*[2,62] Also in this case, our remarks concerning the absolute energy position of the calculated bands apply. Again, the agreement between theory and experiment would be further improved if one shifted the calculated bands rigidly down by $\Delta E = 0.2$ eV.

C. S:Si(001)-(1×1) and Se:Si(001)-(1×1)

Group-VI elements are adsorbed on Si(001) in twofold coordinated sites, as can be expected from simple chemical considerations. We have carried out energy minimizations for the chemisorption of S and Se setting out from several start geometries within (2×1) or (1×2) symmetry. In all cases we arrived at the same (1×1) equilibrium configuration where the S (Se) atoms are adsorbed in bridge positions above the topmost Si atoms. All of the adatoms are fully coordinated. Structurally, these chemisorption systems are very close to the ideal bulk-terminated Si(001) surface. The three topmost layers are shifted slightly by (−0.174 Å, −0.028 Å, 0.005 Å) for S:Si(001) and by (0.075 Å, 0.017 Å, 0.006 Å) for Se:Si(001) with respect to the positions of the ideal lattice planes. Electronically, however, there are distinct differences between these chemisorption systems and the ideal Si(001) surface. Figure 8 shows the surface band structure for Se:Si(001)-(1×1) as resulting from our Green's-function calculation for the optimized geometry. The characteristic fingerprints of the Se chemisorption are the bands labeled S, B_1, D, and B_{bri}. Their wave-vector-resolved charge densities at K are shown in Fig. 9. The band S derived from the Se s states resides in energy below the Si bulk bands. The p-like band B_1 stems from the Se-Si chemisorption bonds. The dangling bonds of the selenium adatoms give rise to the dangling-bond band D and the related antibonding band D^*. The remaining lone-pair orbitals of Se act like bridges between second-nearest-neighbor Se atoms along the [−110] direction. Their interaction gives rise to the band B_{bri}. The bands D and B_{bri} are completely filled since each Se atom has

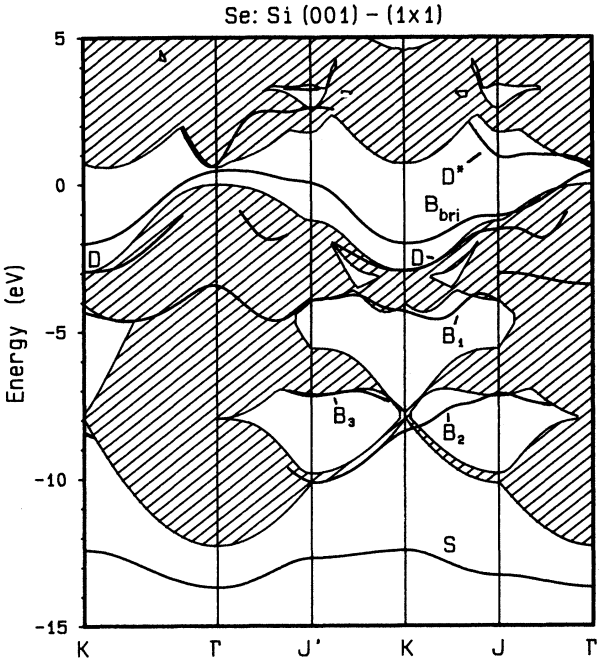

FIG. 8. Surface band structure of Se:Si(001)-(1×1).

six valence electrons. A (2×1) reconstruction by dimerization would not yield any energy gain and thus does not occur for Se:Si(001). This is in marked contrast to the ideal Si(001) surface, where the corresponding bridge-bond and dangling-bond bands reside higher in energy due to the weaker Si potential, as compared to Se, and overlap within the bulk gap. These bands at the clean surface are filled partially only, leading to a metallic surface which is unstable against a (2×1) reconstruction. The S:Si(001) chemisorption system behaves, for obvious reasons, very similarly to Se:Si(001). Its band structure is, as well, very similar to the Se:Si(001) band structure, with deviations of up to 0.5 eV.

Bringans and Olmstead have observed a (1×1) LEED pattern for thin Se films on Si(001) after a careful preparation procedure.[3] However, from their core-level spectra they concluded that one half of the topmost Si atoms are bonded to two Se atoms and the other half is bonded to one Se atom. This would be consistent with $\frac{3}{4}$ of a monolayer of Se atoms in bridge positions. Detailed ARPES measurements have not been reported for this system. Weser *et al.*[26] have investigated S:Si(001) experimentally. They have not observed an ordered S adlayer. It is not clear whether this is a consequence of their preparation technique. The same authors have obtained S:Ge(001) in a well-ordered (1×1) configuration.[23] We have discussed the properties of that system on the basis

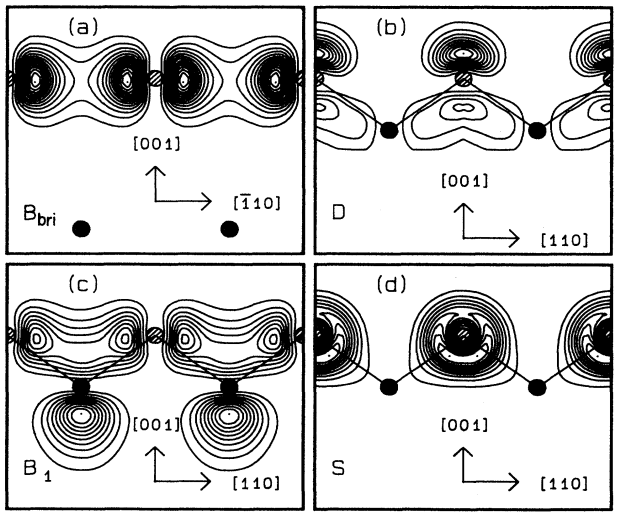

FIG. 9. Energy-resolved charge-density contours of localized states at the K point for Se:Si(001)-(1×1).

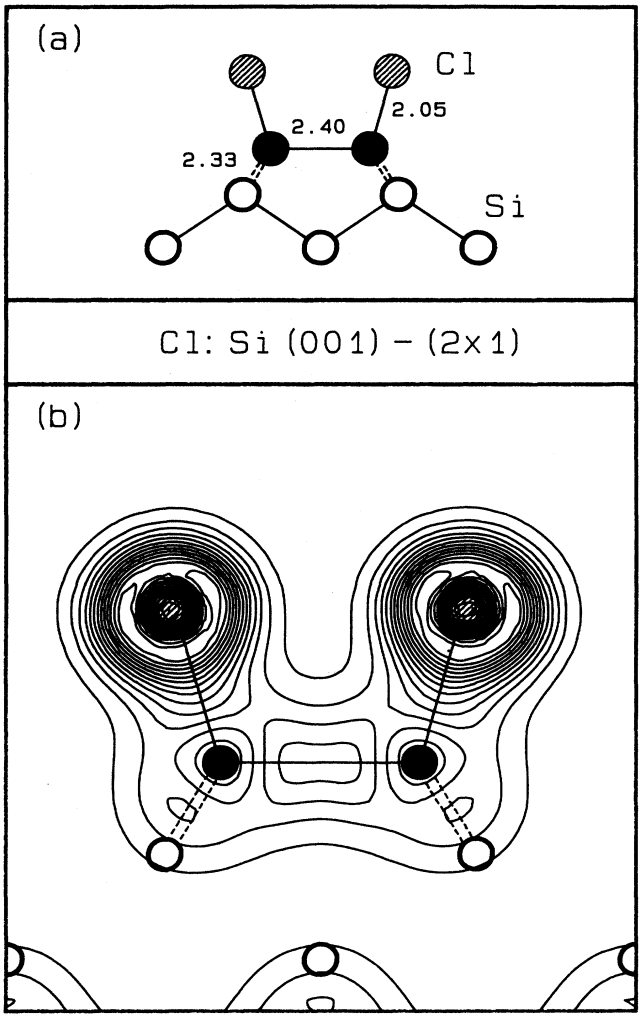

FIG. 10. (a) Side view of the Cl:Si(001)-(2×1) symmetric dimer geometry. The bond lengths are given in angstroms. (b) Total valence charge-density contours of Cl:Si(001)-(2×1) plotted in a [001]-[1$\bar{1}$0] plane.

of first-principles Green's-function calculations in Ref. 25. The resulting surface band structure is very similar to the band structure shown in Fig. 8. Especially, the corresponding bands B_1 and D seem to have been observed for S:Ge(001) by ARPES measurements.[24]

Recently, Kaxiras[63] studied the S:Si(001) and Se:Si(001) chemisorption systems using LDA slab calculations. His results are very close to ours. In addition, he has shown that these restored surfaces are stable against structural changes such as embedding the adsorbates in subsurface sites.

D. Cl:Si(001)-(2×1)

The optimal structure and the total valence charge density as resulting from our calculations for the adsorption of a monolayer of Cl atoms on Si(001) shown in Fig. 10. The Cl atoms are adsorbed at the dangling bonds of the clean surface. The Si-Si dimers become symmetric with a dimer-bond length of 2.40 Å. The Cl-Si bonds are tilted outwards at an angle of 15° to the surface normal with a bond length of 2.05 Å. The back-bond length is 2.33 Å. The calculated binding energy is 4.14 eV per Cl atom. Thornton *et al.*[33] have investigated the Cl:Si(001) binding geometry by SEXAFS measurements. They determined a bond length of 1.95±0.04 Å. A determination of the tilt angle was not possible with the same accuracy. The authors concluded that their data are consistent with a tilt angle of somewhat less than 25°. Recently, Craig and Smith[36] carried out slab MINDO calculations for Cl:Si(001). They obtained an adsorption geometry nearly identical to ours. In addition to this, they have determined another bonding geometry which turns out to be 0.61 eV per surface dimer lower in energy than the symmetric dimer geometry discussed above. In their lower-energy configuration, shown in Fig. 11, the Cl atoms are adsorbed in asymmetric bridge sites. We have investigated this geometry, as well, and we have indeed found a local-energy minimum in configuration space corresponding to the adsorption geometry shown in Fig. 11. In striking difference to the results of Craig and Smith, we find that this configuration is 0.96 eV per dimer *higher* in energy with respect to the symmetric dimer geometry (see *Note added in proof*). Also, from chemical considerations, adsorption in bridge sites would be very astonishing for Cl:Si(001).

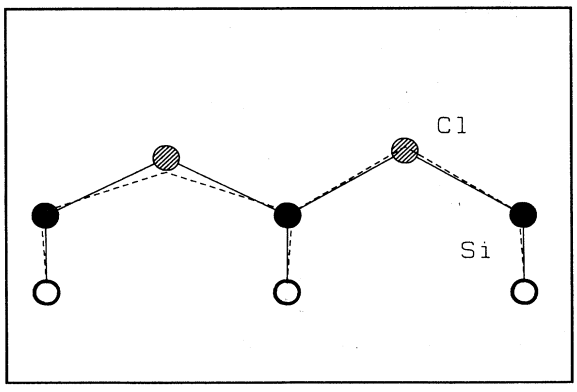

FIG. 11. Side view of the Cl:Si(001)-(2×1) "bridge geometry" as resulting from our calculation. The dashed line indicates the bonding geometry determined in Ref. 36.

In Fig. 12 the surface band structure for the optimal symmetric dimer configuration (see Fig. 10) is shown. The Cl 3*s* and 3*p* orbitals give rise to many surface states and resonances. We have labeled the states according to their physical origin. The corresponding energy- and wave-vector-resolved charge densities are shown in Fig. 13. Before we discuss these results, it is instructive for a better understanding of the origin of these states to consider a rather idealized system first: the adsorption of a single Cl atom at an isolated sp^3 orbital which represents a Si dangling-bond orbital. This is illustrated in Fig. 14(a) where we have introduced a coordinate system with x in $[-110]$ direction and y in [110] direction. To ease the discussion of the isolated Cl-Si "molecules" it is convenient to use two additional coordinate system with axes (1,2,3) and (1′,2′,3′) respectively, parallel or perpendicular to the Cl-Si bonds, as indicated in Fig. 14(a). The energy levels of a free Cl atom and an sp^3 orbital, as well as of the coupled system, are shown in Figs. 14(b) and 14(c), respectively. The state with the lowest energy is mainly Cl *s*-like due to the large energetic separation of Cl 3*s* and Cl 3*p* orbitals. The p_2 and p_3 levels do not couple to the rest due to the symmetry. The remaining orbitals are p_1, sp^3 bonding and antibonding states with a small Cl *s* admixture. The antibonding state is empty. Coupling the two Si-Cl molecules in Fig. 14(a) splits all states and removes the degeneracy of the p_2, p_3 levels. We have labeled the eight occupied states by $S_a, \ldots, P_{3b}$ in Fig. 14(d). The main features of the idealized molecule also

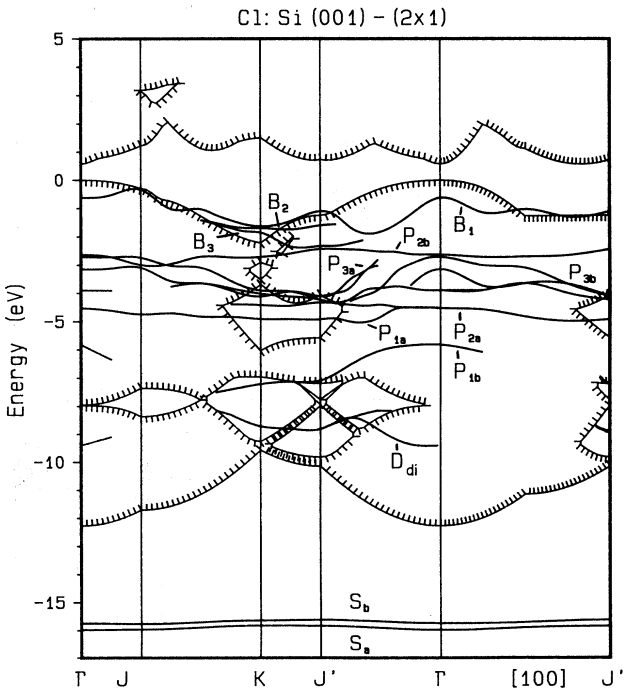

FIG. 12. Surface band structure of Cl:Si(001)-(2×1).

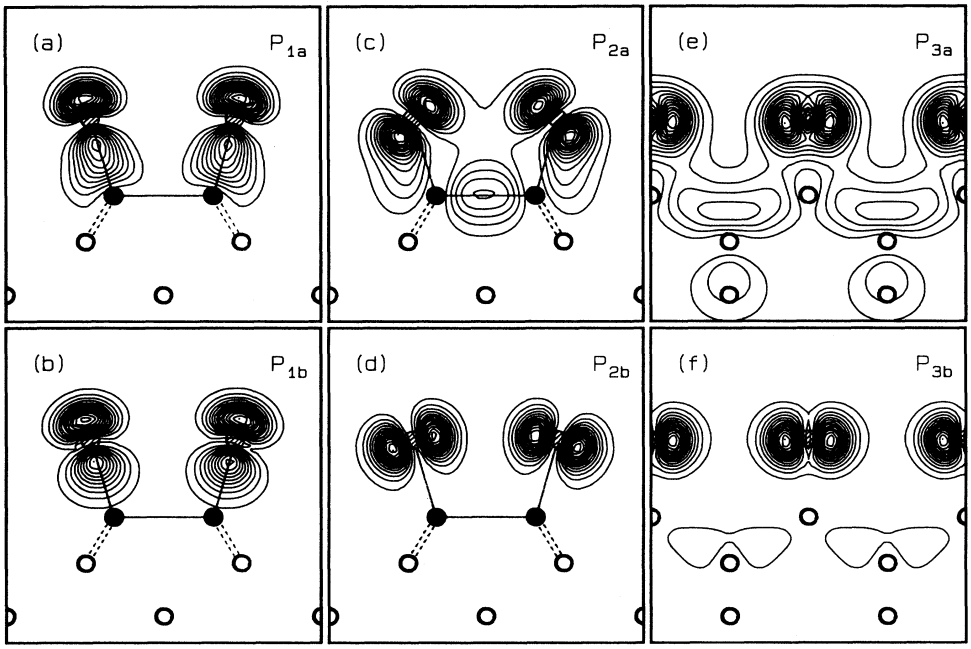

FIG. 13. Energy-resolved charge-density contours of localized states at the $\Gamma J'/2$ point for Cl:Si(001)-(2×1). (a)–(d) are plotted in a [001]-[1$\bar{1}$0] plane containing a Si-Si dimer. (e) and (f) are plotted in a [001]-[110] plane containing a Cl adatom.

appear in the surface band structure for the extended system shown in Fig. 12. At −16 eV there are symmetric and antisymmetric combinations of the Cl s states labeled S_a and S_b. The states at −7 and −5 eV are mainly p_z-like. They correspond to dangling-bond states with their charge maxima outside the crystal in ⟨1⟩ and ⟨1′⟩ directions, as can be seen in Figs. 13(a) and 13(b). The orbitals, whose lobes are directed in ⟨2⟩ direction at the first Cl atom and ⟨2′⟩ direction at the second Cl atom [see Fig. 14(a)] give rise to the band P_{2b}. Its charge density is shown in Fig. 13(d). For the band P_{2a} the situation is more complicated due to a coupling of this state with the Si-Si back bonds. The bands P_{3a} and P_{3b} stem from the Cl p_y orbitals which form bridge bonds between the Cl atoms [see Figs. 13(e) and 13(f)]. They are separated by a second-nearest-neighbor bulk distance. The band D_{di} stems from the interaction of the Cl dangling bonds with the Si-Si dimer bond. Charge-density relaxations near the Si atoms due to the chemisorption give rise to the back-bond bands B_1–B_3. The electrons belonging to these states are mainly localized between the second and third layers.

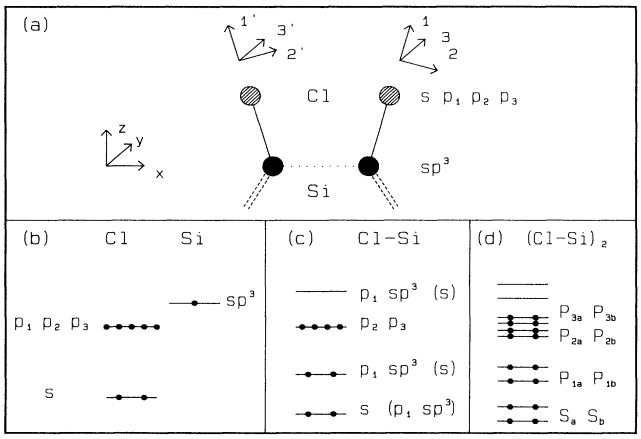

FIG. 14. (a) Side view of two hypothetical Cl-Si (sp_3) molecules. Energy levels for (b) a free Cl atom and a single Si sp_3 orbital, (c) a single Cl-Si (sp_3) molecule and (d) two interacting molecules. In this simple picture the interaction with the dimer bond [dotted line in (a)] and the back bonds [dashed lines in (a)] is not taken into account.

From the experience with other chemisorption systems we expect that the Cl dangling-bond states are the predominant candidates to be detected in photoemission measurements. Johansson *et al.* have obtained in their ARPES measurements[4] pronounced Cl-induced features in the energy range from −4 to −7 eV below the valence-band maximum. The measurements have been carried out with light that was polarized parallel ($A_{\parallel}$) or perpendicular ($A_{\perp}$) with respect to the plane of incidence to investigate the symmetry properties of the states. Johansson *et al.* have determined from their experimental data empirical dispersions of the Cl-induced states.[4] All measured bands have rather small dispersions (< 0.5 eV). Our calculations show that the interaction between the Cl dangling-bond orbitals gives rise to the bands P_{1a} and P_{1b} with a dispersion of 1 eV along Γ-J'. The calculated bands P_{2a} and P_{2b} have a rather small dispersion which would be compatible with the experimental data. However, the absolute energetic position and the energy separation between P_{2a} and P_{2b} are not compatible with

the experimental findings. In addition to this, no peak structures have been resolved in the ARPES measurements above -4 eV, where an emission from the Cl p_y orbitals would be expected from the calculation. We are not able to give a conclusive interpretation of the ARPES data with flat surface bands for Cl:Si(001)-(2×1) on the basis of our calculations. This situation calls for a detailed analysis of the experimental data with respect to symmetry and intensity of the various features in direct comparison with the theoretical results on symmetry and wave-function character of the various states. This analysis will be carried out in the near future.

E. Discussion

Table II compiles the calculated Si-adatom bond length, the ionization energy, and the binding energy for the different chemisorption systems studied in this paper in comparison with the covalent radii. At the clean Si(001)-(2×1) surface, the topmost atoms are threefold coordinated, which is not the optimal configuration for this "four-electron system." Buckling of the dimers reduces the total energy. It is interesting to note that addition of one electron per Si-dimer atom (no additional proton) leads to a more symmetric dimer configuration.[15,64] Badziag, Verwoerd, and Van Hove[64] have suggested that this unbuckling by additional electrons which may be induced by a STM tip is a possible explanation why symmetric dimers are observed in the STM images of Si(001)-(2×1). In the case of As chemisorption these additional electrons are already incorporated in a "natural way." The resulting equilibrium geometry consists of symmetric As-As dimers. The As-Si back-bond length is larger than the Si-Si back-bond length at the clean surface, in accordance with the ratio of the covalent radii of Si and As. The As adatoms in the dimers are threefold coordinated, as in the case of bulk As. Twofold-coordinated adsorption is most favorable for chemisorption of S or Se at Si(001), as our calculations show. The adatom-Si bond lengths follow the trend of the corresponding covalent radii. S bonds stronger to Si(001) than Se. However, this is not an indication that S will grow on Si(001) as a well-ordered monolayer. Total-energy differences to $SiSe_2$ films and enthalpy effects have to be estimated to clarify this point. This is beyond the limit of the present calculational scheme. The calculated binding energy of 2.6 eV per bond for a well-ordered S layer is in agreement with the Si-S bond energy of 2.35 eV estimated by Pauling.[65] One should keep in mind that overestimation of binding energies is a well-known effect of the LDA.

Cl atoms are chemisorbed at the Si-Si dimers in onefold-coordinated sites. The Cl-Si bond length of 2.05 Å is very close to the bond length in the $SiCl_4$ molecule (2.02±0.02 Å). These bond lengths are considerably shorter than the sums of the covalent radii (2.16 Å for Si-Cl). Pauling[65] claimed that the strong ionic character of the bond and an additional π bonding is responsible for this "partial double bond." The same phenomenon has been observed for the chemisorption of Cl at Si(111). Bachelet and Schlüter[66] have estimated a bond length of 2.02 Å from their LDA calculations for Cl:Si(111), in excellent agreement with the results of SEXAFS measurements (2.03±0.03 Å) carried out by Citrin, Rowe, and Eisenberger.[67] We have calculated a binding energy of 4.14 eV per bond for the well-ordered Cl monolayer on Si(001). The binding energy in the $SiCl_4$ molecule is 3.73 eV per bond.[65]

Finally, we will comment on trends in the energetic position of the adatom-induced states for the different chemisorption systems. We will restrict ourselves to a discussion of the characteristic dangling-bond and *s*-like states. Table III shows the calculated LDA eigenenergies for the *s* and *p* states of isolated atoms. The energy scale refers to the vacuum level. Dangling-bond-state (D) and *s*-state (S) energies at $\mathbf{q}=(a,0,0)/2$ are given in the second column of Table III for the different chemisorption systems. These energies are referred to the valence-band maximum of bulk Si. Comparing the *absolute* positions of the atomic levels and the band values the ionization energy has to be subtracted from the band values. The energetic positions of the *s* states decrease nearly monotonically with increasing number of valence electrons of the adsorbed species. The shift of the dangling-bond states is smaller due to their interaction with the bulk states.

IV. SUMMARY AND CONCLUSIONS

In this paper we have investigated the properties of ordered monolayers of group-IV to group-VII elements on Si(001). The clean Si(001) surface shows a (2×1) reconstruction by forming Si-Si dimers which are buckled, as

TABLE II. Summary of calculated bond lengths, ionization energies, and binding energies per atom. The covalent radii are taken from Ref. 65.

Adsorbate	Si-adsorbate bond length (Å)	Dimer bond length (Å)	Covalent radius (Å)	Ionization energy (eV)	Binding energy (eV)
Si	2.33/2.28	2.25	1.17	4.11	5.07
As	2.42	2.52	1.21	4.36	5.44
S	2.23		1.04	5.33	5.20
Se	2.37		1.17	4.59	4.73
Cl	2.05	2.40	0.99	5.20	4.14

TABLE III. Eigenvalues for s and p valence states of free atoms resulting from a local-density approximation (LDA) calculation. These values are compared with the calculated energies of the s-like states (S) and dangling-bond states (D) of the clean Si(001)-(2×1) surface and different adatom:Si(001) chemisorption systems.

	Atomic LDA values (eV)		Chemisorption system (eV)	
Absorbate	E_s	E_p	S	D
Si	−10.88	−4.17	−11.3	−0.2
As	−14.67	−5.53	−12.1	−0.9
S	−17.27	−7.11	−13.3	−2.2
Se	−17.45	−6.92	−13.0	−2.1
Cl	−20.67	−8.79	−16.0	−2.7

of As breaks these dimers and adds As-As dimers on top. This process induces As dangling-bond and dimer-bond states whose calculated dispersions are in excellent agreement with photoemission data. For the adsorption of S and Se we have obtained optimal configurations with bridge positions as adsorption sites within a (1×1) symmetry. This corresponds to a restoration of the ideal bulk-terminated geometry. Our calculations rule out adsorption geometries with (2×1) or (1×2) symmetry, in agreement with experiment. However, the real adsorption process is more complicated due to the formation of SiS_2 or $SiSe_2$ films, respectively. There are indications[3] that ordered (1×1) Se monolayers can be grown by careour calculations show. The electronic structure compares well with the experimental spectra. Chemisorption ful preparation techniques. Cl atoms finally adsorb at the dangling bonds of the Si dimers, which become symmetric upon chemisorption. The Si-Cl bonds are tilted 15° outwards with respect to the surface normal. This configuration, obtained as a minimum of the total energy in our calculation, is consistent with the results of SEXAFS experiments. The computed surface band structure is in poor agreement with the surface-state bands as determined from recent ARPES data. The photoemission experiments show features without dispersion which cannot be easily reconciled with our calculated bands for the dimer adsorption model.

Note added in proof. The authors of Ref. 36 have recently informed us that their MINDO codes used for the calculations reported in Ref. 36 contained an error. After correcting it, they find that their calculations yield the lowest energy configuration for a monolayer of Cl adsorbed at Si(001)-(2×1), when the Cl adatoms are adsorbed on top of the Si dangling bonds of the symmetric Si dimers. This configuration turns out to be 0.75 eV per adatom lower in energy than their bridge geometry (see Fig. 11).

ACKNOWLEDGMENTS

We thank Dr. A. Mazur for numerous helpful discussions. One of us (P.K.) gratefully acknowledges support from the Bennigsen-Foerder-Programm of Northrhine-Westfalia.

[1]R. D. Bringans, in *Angle-Resolved Photoemission,* edited by S. D. Kevan (Elsevier, Amsterdam, 1990).
[2]R. D. Bringans, R. I. G. Uhrberg, R. Z. Bachrach, and J. E. Northrup, Phys. Rev. Lett. **56**, 520 (1986).
[3]R. D. Bringans, and M. A. Olmstead, Phys. Rev. B **39**, 12 985 (1989).
[4]L. S. O. Johansson, R. I. G. Uhrberg, R. Lindsay, P. C. Wincott, and G. Thornton, Phys. Rev. B **42**, 9534 (1990).
[5]R. E. Schlier and H. E. Farnsworth, J. Chem. Phys. **30**, 917 (1959).
[6]Y. Enta, S. Suzuki, and S. Kono, Phys. Rev. Lett. **65**, 2704 (1990).
[7]For reference see, e.g., D. Haneman, Rep. Prog. Phys. **50**, 1045 (1987); M. Schlüter, in *The Chemical Physics of Solid Surfaces and Heterogeneous Catalysis,* edited by D. A. King and D. P. Woodruff (Elsevier, Amsterdam, 1988), Vol. 5, p. 37.
[8]D. J. Chadi, Phys. Rev. Lett. **43**, 43 (1979).
[9]R. M. Tromp, R. G. Smeenk, and F. W. Saris, Phys. Rev. Lett. **46**, 9392 (1981).
[10]M. Aono, Y. Hou, C. Oshima, and Y. Ishizawa, Phys. Rev. Lett. **49**, 567 (1982).
[11]B. W. Holland, C. B. Duke, and A. Paton, Surf. Sci. **140**, L269 (1984).
[12]M. T. Yin and M. L. Cohen, Phys. Rev. B **24**, 2303 (1981).
[13]K. C. Pandey, in *Proceedings of the 17th International Conference on the Physics of Semiconductors,* edited by J. D. Chadi and W. A. Harrison (Springer, Berlin, 1984).
[14]Z. Zhu, N. Shima, and M. Tsukada, Phys. Rev. B **40**, 11 868 (1989).
[15]J. Dabrowski and M. Scheffler, Appl. Surf. Sci. **56**, 15 (1992).
[16]K. Kobayashi, Y. Morikawa, K. Terakura, and S. Blügel, Phys. Rev. B **45**, 3469 (1992).
[17]M. C. Payne, N. Roberts, R. J. Needs, M. Needels, and J. D. Joannopoulos, Surf. Sci. **211/212**, 1 (1989).
[18]I. P. Batra, Phys. Rev. B **41**, 5048 (1990).
[19]E. Artacho and F. Yndurain, Phys. Rev. Lett. **62**, 2491 (1989).
[20]S. Tang, A. J. Freeman, and B. Delley, Phys. Rev. B **45**, 1776 (1992).
[21]R. J. Hamers, R. M. Tromp, and J. E. Demuth, Phys. Rev. B **34**, 5343 (1986).
[22]R. A. Wolkow, Phys. Rev. Lett. **68**, 2636 (1992).
[23]T. Weser, A. Bogen, B. Konrad, R. D. Schnell, C. A. Schug, and W. Steinmann, Phys. Rev. B **35**, 8184 (1987).
[24]T. Weser, A. Bogen, B. Konrad, R. D. Schnell, C. A. Schug, W. Moritz, and W. Steinmann, Surf. Sci. **201**, 245 (1988).
[25]P. Krüger and J. Pollmann, Phys. Rev. Lett. **64**, 1808 (1990).
[26]T. Weser, A. Bogen, B. Konrad, R. D. Schnell, C. A. Schug, and W. Steinmann, in *Proceedings of the 18th International Conference on the Physics of Semiconductors* edited by O. Engström (World Scientific,, Singapore, 1987), p. 97.
[27]R. D. Bringans, R. I. G. Uhrberg, R. Z. Bachrach, and J. E. Northrup, Phys. Rev. Lett. **55**, 533 (1985).
[28]R. I. G. Uhrberg, R. D. Bringans, M. A. Olmstead, R. Z. Bachrach, and J. Northrup, Phys. Rev. B **35**, 3945 (1987).
[29]P. Krüger, in *Festkörperprobleme,* edited by U. Rössler (Vieweg, Braunschweig, 1991), Vol. 31, p. 133.
[30]S. Ciraci, R. Butz, E. M. Oellig, and H. Wagner, Phys. Rev. B **30**, 711 (1981).
[31]L. S. O. Johansson, R. I. G. Uhrberg, and G. V. Hansson, Phys. Rev. B **38**, 13 490 (1988).

[32]J. E. Rowe and G. Margaritondo, Phys. Rev. B **16**, 1581 (1977).
[33]G. Thornton, P. L. Wincott, R. McGrath, I. T. McGovern, F. M. Quinn, D. Norman, and D. D. Vvedensky, Surf. Sci. **211/212**, 959 (1989).
[34]N. Aoto, E. Ikawa, and Y. Kurogi, Surf. Sci. **199**, 408 (1988).
[35]R. B. Jackman, H. Ebert, and J. S. Foord, Surf. Sci. **176**, 183 (1986).
[36]B. I. Craig and P. V. Smith, Surf. Sci. **262**, 235 (1992).
[37]P. Hohenberg and W. Kohn, Phys. Rev. **136**, B864 (1964).
[38]For reference see, e.g., W. Kohn and P. Vashishta, in *Theory of the Inhomogeneous Electron Gas,* edited by S. Lundqvist and W. H. March (Plenum, New York, 1983).
[39]P. Krüger, A. Mazur, J. Pollmann, and G. Wolfgarten, Phys. Rev. Lett. **57**, 1468 (1986).
[40]P. Krüger and J. Pollmann, Phys. Rev. B **38**, 10 578 (1988).
[41]W. Kohn and L. J. Sham, Phys. Rev. **140**, A1133 (1965).
[42]P. Krüger and J. Pollmann, Physica B **172**, 155 (1991).
[43]We have used orbitals with decay constants of 0.19 and 0.5 for Si bulklike atoms, whereby lengths are measured in atomic units. For surface atoms we have used the following decay constants: Si, As (0.19,0.5,0.8); S, Se (0.19,0.7,1.2); and Cl (0.19,0.6,2.0).
[44]G. B. Bachelet, D. R. Hamann, and M. Schlüter, Phys. Rev. B **26**, 4199 (1982).
[45]D. M. Ceperley and B. J. Alder, Phys. Rev. Lett. **45**, 566 (1980).
[46]J. P. Perdew and A. Zunger, Phys. Rev. B **23**, 5048 (1981).
[47]R. Stumpf, X. Gonze, and M. Scheffler (unpublished).
[48]F. D. Murnaghan, Proc. Natl. Acad. Sci. USA **30**, 244 (1944).
[49]X. Zhu, S. Fahy, and S. G. Louie, Phys. Rev. B **39**, 7840 (1989).
[50]E. P. Wigner, Phys. Rev. **46**, 1002 (1934).
[51]*Numerical Data and Functional Relationships in Science and Technology,* edited by K. H. Hellwege and O. Madelung, Landolt-Börnstein, New Series, Group III, Vol. 17a (Springer, Berlin, 1982).
[52]For a review see G. V. Hansson and R. I. G. Uhrberg, Surf. Sci. Rep. **9**, 197 (1988).
[53]L. S. O. Johansson, R. I. G. Uhrberg, P. Martensson, and G. V. Hansson, Phys. Rev. B **42**, 1305 (1990).
[54]R. D. Bringans, R. I. G. Uhrberg, M. A. Olmstead, and R. Z. Bachrach, Phys. Rev. B **34**, 7447 (1986).
[55]Y. Enta, S. Suzuki, S. Kono, and T. Sakamoto, J. Phys. Soc. Jpn. **59**, 657 (1990).
[56]E. Landemark, R. I. G. Uhrberg, P. Krüger, and J. Pollmann, Surf. Sci. Lett. **236**, L359 (1990).
[57]J. Pollmann, Solid State Commun. **34**, 587 (1980).
[58]P. Feibelman, Phys. Rev. B **35**, 2626 (1987).
[59]G. Wachutka, A. Fleszar, F. Maca, and M. Scheffler, J. Phys. Condens. Matter. **4**, 2831 (1992).
[60]R. S. Becker, T. Klitsner, and J. S. Vickers, J. Microsc. **152**, 157 (1988).
[61]O. L. Alerhand, J. Wang, J. D. Joannopoulos, and E. Kaxiras, J. Vac. Sci. Technol. B **9**, 2423 (1991).
[62]R. I. G. Uhrberg, R. D. Bringans, R. Z. Bachrach, and J. E. Northrup, J. Vac. Sci. Technol. A **4**, 1259 (1986).
[63]E. Kaxiras, Phys. Rev. B **43**, 6824 (1991).
[64]P. Badziag, W. S. Verwoerd, and M. A. Van Hove, Phys. Rev. B **43**, 2058 (1991).
[65]L. Pauling, *The Nature of the Chemical Bond* (Cornell University Press, Ithaca, 1980).
[66]G. B. Bachelet and M. Schlüter, Phys. Rev. B **28**, 2302 (1983).
[67]P. H. Citrin, J. E. Rowe, and P. Eisenberger, Phys. Rev. B **28**, 2299 (1983).